Theory of Speckle-Pattern Tomography in Multiple-Scattering Media

Richard Berkovits and Shechao Feng[a]
Department of Physics, University of California, Los Angeles, California 90024
(Received 31 August 1990)

We develop the principle of "speckle-pattern tomography" in the multiple-scattering regime, i.e., the technique of using correlations between complex interference patterns to determine the position of a special scatterer for either electromagnetic or acoustical wave propagation through a diffusive scattering medium. We focus on two concrete examples which are relevant to experiments and possible applications: (i) detecting the position of a stationary special scatterer in a medium of moving scatterers; (ii) detecting the appearance and position of a new added scatterer.

PACS numbers: 42.20.−y

How can one detect the appearance and the position of a new microcrack in a metal which already contains many such defects, using ultrasonic nondestructive testing techniques? How can one trace the position of a slow-moving particle in a fluid which contains a high density of fast-moving scatterers (such as in a milk), using optical waves? Is it possible to detect the motion of a far-away airplane which is separated from the radar detectors by thick clouds which scatter the radar signal rather strongly? Such are the possible real-life applications of a principle that we formulate in this Letter, namely, the principle of speckle-pattern tomography in the multiple-scattering regime.

Imaging of a special object in a *weak*-scattering medium by means of passing a probing wave through it goes back as far as human eyes could see. In scientific terms, this is most conveniently described by the Born (or single-scattering) approximation in standard scattering theory, a simple example of which we illustrate in Fig. 1(a). Let us suppose a plane wave is incident onto a slab-shaped medium which is assumed to be free of absorption, i.e., the rate of absorption $1/\tau_a$ is much less than the inverse time it takes the wave to pass through the slab, c/L (c is the wave velocity.) This wave can be thought of as either an electromagnetic or an acoustical wave; for simplicity we shall ignore the vector nature of these waves, and use a *scalar* approximation to describe our principle. Assuming in addition that the inhomogeneities in the slab give rise to only weak elastic scattering of the incident wave, characterized by a wave transport mean free path $l^* \gg L$, then it is clear that most of the incident wave remains unscattered upon exiting the slab, whereas the scattered wave, which has an overall intensity much smaller than the unscattered beam, consists of at most contributions from *single*-scattering events, and the scattering by a special object located at $\mathbf{r}_0$, which let us say scatters the wave more strongly than the other scatterers, gives rise to a spherical (scattered) wave which forms the image of this object to the right of the sample. Without loss of generality, we shall assume throughout our discussion that the inhomogeneities in the scattering medium can be described by pointlike scatterers with a concentration n_s; then l^* is given by $l^* = 1/n_s\sigma^*$, where $\sigma^* = \int \sigma(\theta)(1-\cos\theta)d\Omega$ is the transport scattering cross section for each scatterer. We

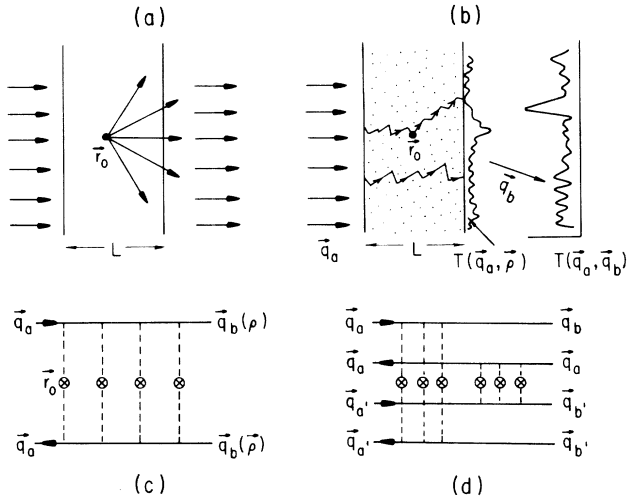

FIG. 1. (a) Illustration of imaging in the single-scattering regime $L \ll l^*$. Most of the incident plane wave propagates through the sample unscattered; the spherical scattered wave due to the special scatterer placed at $\mathbf{r}_0$ forms the image of this object on the right of the sample. (b) Illustration of the principle of tomography of the position of a special scatterer in the multiple-scattering regime $L \gg l^*$. Here the entire transmitted beam is the result of multiple scattering in the sample; the typical number of scattering events for any partial wave is $\sim (L/l^*)^2$. $T(\mathbf{q}_a,\mathbf{q}_b)$ is the intensity transmission coefficient in a far-field screen which is placed at a distance $d \gg L$ from the right-hand side of the slab-shaped sample. $T(\mathbf{q}_a,\boldsymbol{\rho})$ is the near-field intensity transmission coefficient, collected by a screen placed on the right face of the sample. When averaged over the positions of all the scatterers in the sample except the special one placed at $\mathbf{r}_0$, these transmission coefficients (or their correlation functions) contain information about the position of the stationary scatterer $\mathbf{r}_0$. (c) Feynman diagram for calculating the average far-field (near-field) intensity transmission coefficient with a stationary scatterer placed at $\mathbf{r}_0$. (d) Feynman diagram for calculating the correlation function $C_{aba'b'} = \langle \delta T(\mathbf{q}_a,\mathbf{q}_b)\delta T(\mathbf{q}_{a'},\mathbf{q}_{b'})\rangle$, again for the case of a stationary scatterer fixed at $\mathbf{r}_0$.

thus see that tomography, or in this case simply imaging, of a special scatterer can be achieved easily in the Born or single-scattering regime. Most present-day imaging techniques are based on such a simple principle.[1]

We now focus on the opposite *strong-* or *multiple-scattering* regime $l^* \ll L$ (but still in the weak-localized regime $\lambda \ll l^*$). As illustrated in Fig. 1(b), the plane wave which is incident onto the left side of the slab must in this case scatter *multiply* in traversing the sample, i.e., all the partial waves must *diffuse* across the sample, with a typical number of scattering events being of the order $(L/l^*)^2$. The unscattered beam in this case is exponentially attenuated, by a factor e^{-L/l^*}. The outgoing-wave intensity pattern will in this case be a complicated interference pattern, which is often known as a *speckle pattern*. Suppose a special strong scatterer is again placed at $\mathbf{r}_0$; it is clear that no simple image of this object shall be formed on the screen. Is it then still possible to use the information contained in the complex interference speckle pattern to locate the position of this special scatterer? From a fundamental point of view this should be possible, as the speckle-pattern intensity as a function of angle or frequency is uniquely determined by the positions of *all* the scatterers in the system, i.e., it is a kind of "fingerprint" of the positions of all the scatterers in the sample. Thus, it might still be possible to retrieve some important information about the location of the special scatterer, thus allowing one to perform *tomography* in a random-scattering medium in the multiple-scattering limit. This is precisely what we set out to do in this Letter.

We shall assume in our subsequent discussions that absorption can still be regarded as negligible even in the multiple-scattering limit, i.e., we require that $1/\tau_a \ll D/L^2$, where $D = cl^*/3$ is a diffusion constant which characterizes the random-walk-like multiple-scattering process of the wave propagation. We make this requirement simply because if a random-scattering medium is strongly absorbing, then no information about the scatterer positions will be transmitted through the slablike sample, and tomography in this case will not be possible. The effect of weak absorption can be easily incorporated into our theoretical framework, and this will be done elsewhere due to space limitations.

The easiest experimentally measurable quantity relevant to our discussion is the far-field intensity transmission coefficient $T(\mathbf{q}_a, \mathbf{q}_b)$, which is defined as the intensity in direction $\mathbf{q}_b$ on the far right-hand side of the sample, if the unit-flux incident wave is in a direction $\mathbf{q}_a$ on the left-hand side [see Fig. 1(b)]. Here $\mathbf{q}$ is the transverse wave vector for the wave function outside the disordered sample (on either side), satisfying the conservation relation $\mathbf{q}^2 + k_z^2 = k_0^2 = (\omega/c)^2$, with the z direction being the normal to the slab. From the point of view of tomography, it is even better to have the *near-field* intensity transmission coefficient, $T(\mathbf{q}_a, \boldsymbol{\rho})$, where $\boldsymbol{\rho}$ is the transverse spatial coordinates on the right face of the slablike sample, as it contains more direct information about the position of a special scatterer. But it may not be easily attainable in realistic experimental situations, as the near-field speckle-pattern intensities vary on length scales of the wavelength λ, which is sometimes difficult to resolve with simple photon detectors.

Coherent diffusive (i.e., multiply scattered) wave transport has been at the heart of many recent advances in the so-called "mesoscopic physics." A few well-known examples include the weak-localization effect,[2] the universal conductance fluctuations,[3] the extreme sensitivity to impurity motions, and the anomalous $1/f$ noise in the context of the transport properties of low-temperature electronic systems;[4] as well as the diffusive wave spectroscopy,[5,6] the enhanced backscattering peak,[5,7] the long-range correlations, and the "memory effect"[8] in the context of optical wave propagation through disordered scattering medium. In a particularly related work, the idea of using correlation functions in the magnetoconductance fluctuations in a mesosopic metal to determine the position of a two-level tunneling center has been recently proposed by Fal'ko and Kmel'nitskii.[9]

We start by considering the problem of trying to locate a special scatterer which is *fixed* in space at $\mathbf{r}_0$ [see Fig. 1(b)], while the rest of the scatterers (total number M) move around randomly in a multiply scattered random medium. One concrete example in real life is trying to use a laser beam to locate a slow-moving particle immersed in a milklike dense scattering medium where simple images of this special scatterer are totally absent. In this context we define the ensemble average $\langle \cdot \rangle$ to be an average over the M moving scatterer positions, i.e., a simple time average. The important correlator for the scattering potential u in Fourier space is given by

$$\langle u(\mathbf{q},\mathbf{r}_0) u^*(\mathbf{q}',\mathbf{r}_0) \rangle = \frac{4\pi}{Vl^*} \delta(\mathbf{q}-\mathbf{q}') + \frac{u^2}{V^2} e^{i(\mathbf{q}-\mathbf{q}')\cdot\mathbf{r}_0}, \tag{1}$$

where $V = AL$ is the sample volume with A being the cross-sectional area of the slab. From Eq. (1), and using the standard Feynman diagram for the average transmission coefficient in the multiple-scattering regime $L \gg l^* \gg \lambda$ [see Fig. 1(c)], we easily obtain

$$\langle T(\mathbf{q}_a,\mathbf{q}_b,\mathbf{r}_0) \rangle = \frac{3\pi l^*}{k^2 AL} \left\{ 1 + \frac{3l^* L}{A} \left[\left(1 - \frac{z_0}{L} \right) \frac{z_0}{L} - \frac{1}{6} \right] \right\}. \tag{2}$$

Thus we see that the average transmission coefficient depends *explicitly* on the distance of the special stationary scatterer relative to the surface of the slab. This makes it possible to determine the longitudinal position z_0 of the special scatterer by a simple measurement of the average far-field transmitted intensity. If the special scatterer is moving slowly (compared to the motion of

the rest of the scatterers), this expression allows for direct tracking of this special scatterer. From a practical point of view, this method for locating a special scatterer is most useful in the quasi-2D limit, i.e., if $A \sim Ll^*$ (we note that the thickness of the sample is still large compared to λ), so that the z_0-dependent term in Eq. (2) is as large as the constant background term. This extreme sensitivity of the transmitted intensity in quasi-2D systems to adding a *single* stationary scatterer to a fluctuating disordered diffusive scattering system, even at the level of the average transmission coefficient, reflects a general property of coherent multiple scattering in quasi-2D disorder media, in which all random-walking partial waves pass through any given scatterer with a finite probability, independent of the size of the system, provided it remains phase coherent. This effect in fact was the reason for the unusually large magnitudes of low-temperature $1/f$ noise in mesoscopic disordered metal films.[4]

As is shown in Eq. (2), it is only possible to determine the *longitudinal* position of a special scatterer z_0 from the knowledge of the far-field transmitted wave intensity, in the multiple-scattering regime. Let us now consider the average near-field transmitted intensity in the same situation. Using similar diagrammatic techniques [see Fig. 1(c)], we find

$$\langle T(\mathbf{q}_a,\boldsymbol{\rho},\mathbf{r}_0)\rangle = \frac{3l^*}{4\pi L}\left[1+\left(\frac{6}{\pi}F(\mathbf{r}_0)-\frac{2l^*L}{A}\right)\right], \quad (3)$$

where

$$F(\mathbf{r}_0)=\left(1-\frac{z_0}{L}\right)\sum_{n=1}\sin(k_n z_0) \times\sin[k_n(L-l^*)]K_0(k_n|\boldsymbol{\rho}-\boldsymbol{\rho}_0|), \quad (4)$$

and $k_n = n\pi/L$. Thus we see that the average near-field intensity in fact has a peak at the position $\boldsymbol{\rho}=\boldsymbol{\rho}_0$. The form factor $F(\mathbf{r}_0)$ for the case that the special scatterer is close to the right edge of the slab, $z_0/L \sim 1$, may be written as

$$F(\mathbf{r}_0)=(1-z_0/L)\{[(\boldsymbol{\rho}-\boldsymbol{\rho}_0)^2+(L-l^*-z_0)^2]^{-1/2} -[(\boldsymbol{\rho}-\boldsymbol{\rho}_0)^2+(L+l^*+z_0)^2]^{-1/2}\}.$$

The particularly strong ρ dependence of this result in 3D allows for the realistic possibility to locate *completely* the position of a stationary scatterer in a fluctuating multiple-scattering medium, which we regard as a truly interesting result. Again visualizing the situation by the example of a slow-moving scatterer immersed in a milk-like medium, our method predicts that a measurement of the time-averaged intensity on the sample surface, using an averaging time which is long compared to the time scale of the random-moving scatterers but short on that of the slow-moving special scattering center, shall yield directly the position of this special scatterer.

In the case where direct measurement of the near-field transmitted intensity is not possible, say because the detector does not have good enough spatial resolution, and considering the 3D limit where the z_0-dependent term in the average far-field transmission coefficient is too small to allow for realistic detection of the position of the special stationary scatterer, it is still possible to extract the *longitudinal* position of the special scatterer at $\mathbf{r}_0$ by collecting the angular *correlation function* of the far-field transmission coefficient $T(\mathbf{q}_a,\mathbf{q}_b)$. In the absence of a stationary scatterer, i.e., when a complete ensemble average of the scatterer positions is made, the angular correlation function of the far-field transmission coefficients $C_{aba'b'}\equiv\langle\delta T(\mathbf{q}_a,\mathbf{q}_b)\delta T(\mathbf{q}_{a'},\mathbf{q}_{b'})\rangle$ has been computed before, and the dominant contribution to this function (the $C^{(1)}$ term in the notation of Feng *et al.*[8]) contains a momentum-conservation condition, i.e., it is zero unless $\Delta\mathbf{q}_a=\Delta\mathbf{q}_b$ ($\Delta\mathbf{q}_a\equiv\mathbf{q}_a-\mathbf{q}_{a'}$). Upon adding the stationary scatterer at $\mathbf{r}_0$, it is easy to show that such a momentum-conservation law is broken, and the $C^{(1)}$ correlation function becomes finite at all values where $\Delta\mathbf{q}_a\neq\Delta\mathbf{q}_b$ and is explicitly given by

$$C^{(1)}_{aba'b'}=9(l^*L/A)^2\langle T(\mathbf{q}_a,\mathbf{q}_b)\rangle^2 G_{z_0}(\Delta q_a,\Delta q_b), \quad (5)$$

where

$$G_{z_0}(\Delta q_a,\Delta q_b)=\left[\frac{\sinh(\Delta q_a z_0)\sinh[\Delta q_b(L-z_0)]}{\sinh(\Delta q_a L)\sinh(\Delta q_b L)}\right]^2. \quad (6)$$

Since in the absence of a fixed special scatterer this correlation function is identically equal to zero for $\Delta\mathbf{q}_a\neq\Delta\mathbf{q}_b$, and it becomes nonvanishing after the placement of such a scatterer, this cross-correlation technique offers a good way to detect the longitudinal position of the fixed scatterer z_0, even when the near-field intensity information is absent in the 3D case. Experimentally, one can simply fix $\Delta\mathbf{q}_a=0$, i.e., using a single incident beam, record the "snapshots" of the far-field transmitted speckle pattern at different times, and perform digitally the cross correlations of the transmission coefficients for different $\Delta\mathbf{q}_b$'s.

Let us now consider a different situation in which the idea of speckle-pattern tomography could be very useful. Imagine we would like to locate the position of a *new* microcrack in a metal which already contains many such microcracks, due to mechanical stress on the system, by using an ultrasonic nondestructive detection technique. The usual ultrasonic imaging techniques in this limit will not function if the system involved is in the multiple-scattering regime $L \gg l^*$. In this context, it is most convenient to measure the *difference* speckle pattern, i.e., one subtracts the two speckle patterns before and after the addition of a special scatterer at $\mathbf{r}_0$. (In fact, the change in the speckle pattern indicates that one or more new cracks have been created in the sample.) Assuming

that the near-field intensity can be directly measured, the difference average intensity can be similarly calculated to yield

$$\langle \delta T(\mathbf{q}_a,\boldsymbol{\rho},\mathbf{r}_0)\rangle \equiv \langle T(\mathbf{q}_a,\boldsymbol{\rho},\mathbf{r}_0) - T(\mathbf{q}_a,\boldsymbol{\rho})\rangle = \frac{3l^*}{4\pi L}\left[\frac{6}{\pi}F(\mathbf{r}_0) - \frac{2l^*L}{A}\right], \quad (7)$$

where the average is again taken as corresponding to moving all the other M scatterers randomly, and $F(x)$ is given in Eq. (4). We note that this average difference near-field speckle intensity is again peaked at $\boldsymbol{\rho}=\boldsymbol{\rho}_0$, thus allowing one to locate the position of the new crack. In real situations, it may not be possible to make a real average over the positions of the other M scatterers inside the sample, and we claim without a proof that a simple angular average around the peak position of the unaveraged difference speckle pattern may be a good enough approximation to achieve speckle-pattern tomography of the added scatterer.

In summary, we have here laid the theoretical foundation for performing tomography in the multiple- or diffusive-scattering regime using coherent waves, where conventional imaging techniques are not applicable. We find that the recent progress in the conductance-fluctuation theory in mesoscopic metals allows us to give precise, analytical expressions which enable one to locate the position of a special scatterer in a highly scattering medium. Our results are general, and can be used in the context of many different kinds of waves, provided the wave function in question is sufficiently coherent. Experimental verification of the various ideas presented here could lead to realistic applications in a range of different engineering disciplines, such as acoustical detection of defects in metals and other materials, and radar or sonar detection of objects in an highly scattering environment.

We thank B. Spivak and D. Kmel'nitskii for useful discussions. R.B. wishes to thank the Wolfson Foundation for financial support. This work was also supported in part by the ONR, under Grant No. N00014-90-J-1829.

[a]Also at II. Physikalisches Institut, Universität zu Köln, 5000 Köln 41, Federal Republic of Germany.

[1]For a review of related topics, see *Multiple Scattering of Waves in Random Media and Random Surfaces,* edited by V. V. Varadan and V. K. Varadan (Penn State Univ. Press, University Park, 1985).

[2]For a review see P. A. Lee and T. V. Ramakrishnan, Rev. Mod. Phys. **57**, 287 (1985); G. Bergmann, Phys. Rep. **107**, 1 (1984).

[3]R. A. Webb, S. Washburn, C. P. Umbach, and R. B. Laibowitz, Phys. Rev. Lett. **54**, 2696 (1985); J. C. Licini, D. J. Bishop, M. A. Kastner, and J. Melngailis, Phys. Rev. Lett. **55**, 2987 (1985); W. J. Skocpol *et al.*, Phys. Rev. Lett. **56**, 2865 (1986); S. B. Kaplan and A. Harstein, Phys. Rev. Lett. **56**, 2692 (1986); P. A. Lee and A. D. Stone, Phys. Rev. Lett. **55**, 1622 (1985); B. L. Al'tshuler, Pis'ma Zh. Eksp. Teor. Fiz. **41**, 530 (1985) [JETP Lett. **41**, 648 (1985)].

[4]B. L. Alt'shuler and B. Z. Spivak, Pis'ma Zh. Eksp. Teor. Fiz. **42**, 363 (1985) [JETP Lett. **42**, 447 (1986)]; S. Feng, P. A. Lee, and A. D. Stone, Phys. Rev. Lett. **56**, 1960 (1986).

[5]For a review of recent progress in wave propagation in random media, see *Scattering and Localization of Classical Waves in Random Media,* edited by P. Sheng (World Scientific, Singapore, 1990).

[6]D. J. Pine, D. A. Weitz, P. M. Chaikin, and E. Herbolzheimer, Phys. Rev. Lett. **60**, 1134 (1988); G. Maret and P. E. Wolf, Z. Phys. B **65**, 409 (1987); M. J. Stephen, Phys. Rev. B **37**, 1 (1988); A. Z. Genack, Phys. Rev. Lett. **58**, 2043 (1987).

[7]Y. Kuga and A. Ishimaru, J. Opt. Soc. Am. A **4**, 831 (1984); M. P. van Albada and L. Lagendijk, Phys. Rev. Lett. **55**, 2696 (1985); P. E. Wolf and G. Maret, *ibid.* **55**, 2696 (1985); M. Kaveh, M. Rosenbluh, I. Edrei, and I. Freund, *ibid.* **57**, 2049 (1986); P. E. Wolf, G. Maret, E. Akkermans, and R. Maynard, J. Phys. (Paris) **49**, 63 (1988).

[8]B. Shapiro, Phys. Rev. Lett. **57**, 2168 (1986); M. Stephen and G. Cwillich, Phys. Rev. Lett. **59**, 285 (1987); S. Feng, C. Kane, P. A. Lee, and A. D. Stone, Phys. Rev. Lett. **61**, 834 (1988); I. Freund, M. Rosenbluh, and S. Feng, Phys. Rev. Lett. **61**, 2328 (1988); N. Garcia and A. Z. Genack, Phys. Rev. Lett. **63**, 1678 (1989); M. P. van Albada, F. de Boer, and A. Lagendijk, Phys. Rev. Lett. **64**, 2787 (1990).

[9]V. Fal'ko and D. E. Kmel'nitskii, JETP Lett. **51**, 189 (1990).